

Analysis and Reducing Methods of Cogging Torque on Permanent Magnet AC Servo Motor

Chengtao Dang¹, Wei Zhou², Licheng Yin³, Ningze Tong¹

¹ Servo System Design and Research Institution of ARIM, China

² Beijing Martial Delegate Agency

³ Central Iron and Steel Research Institute National Analysis Center for Iron & Steel

E-mail: dctmagician@163.com

Abstract — How to reduce cogging torque of servo motor is a difficult problem in the design, manufacture and application process due to the high requirements of positioning accuracy and performance. In this paper, analysis models of different cogging torque are compared based on the theory of the cogging torque, the method to suppress cogging torque in 6-pole 36-slot motors are summarized, the scheme to optimize cogging torque is given through the design of the prototype. And the effect of the solder bath can not be ignored in the motor design process. Take the 6-pole 36 slot prototype as an example, the effect of factors such as solder bath on the cogging torque is analyzed, the scheme to reduce the effect of solder bath is given according to the comparison.

I. INTRODUCE OF COGGING TORQUE

Permanent magnet synchronous motors (PMSM) are widely used in variety high-performance speed and position control systems. The PMSM inevitably interact with slotted armature iron core because it contains permanent magnet poles, as to produce the cogging torque which cause vibration and noise, affect the operation performance and control accuracy of motor^[1].

The analytical approaches to compute the cogging torque generally have energy method, Maxwell tensor method, and the numerical method. This paper simulates the magnetic field distribution of 6-pole 36-slot motor and based on finite element method, the computed result with the proposed method is closer to the actual value of cogging torque.

II. ANALYSIS OF COGGING TORQUE CALCULATION METHOD

A. Analytical Method of cogging torque

The analytical approaches to compute the cogging torque of motor generally have energy method^[2], Maxwell tensor method^[3], and the numerical method. Cogging torque is calculated using the analytical method followed assumptions^[4], (1)The permeability of armature core tends to infinity, while the permeability of the permanent magnet is similar to air gap; (2)Energy changes of permanent magnet close to 0; (3)Iron core lamination coefficient is similar to 1; (4)The 3-D model is Simplified to the 2-D model, ignoring the ends of the magnetic flux leakage; (5)Excluding the impact of other motor structures.

(i)Energy method

The analysis of cogging torque using energy method is usually based on the change of magnetic permeability. When

the relative movement happens between the permanent magnet poles and the slots of armature, the relative combination position between the slots and permanent magnets will change periodically. Since the permeability of the combination changes as it, the magnetic energy storage in the air gap and the permanent magnet will change, thus the cogging torque is produced.

Cogging torque is expressed as:

$$T_{\text{cog}} = -\frac{1}{2\mu_0} \frac{\partial}{\partial \alpha} \int_V B^2 dV \quad (1)$$

(ii) Maxwell tensor method

Maxwell tensor method uses the equivalent magnetic tension (surface force) to replace the volume force. From the Maxwell electromagnetic field standpoint, the stress is existed in the internal magnetic field. The electromagnetic field of the internal and external unit volume, the stress on the boundary surface can be determined from the stress tensor. According to this principle, the analysis method of cogging torque is deducted by the method of tensor. To find a closed space surface S in the air gap of the motor, the expression of cogging torque can be obtained by the second type of surface integral on it according to Maxwell stress tensor method.

Cogging torque is expressed as:

$$\bar{T}_{\text{cog}} = \frac{1}{\mu_0} \iint_S \left[(\vec{r} \times \vec{B}) (\vec{B} \times \vec{n}) - \frac{1}{2} B^2 (\vec{r} \times \vec{n}) \right] dS \quad (2)$$

Simplified the 3-D model to 2-D model, the space vector will become the plane vector, thus the surface integral along the surface S in the original model will become curve integral. To do the curve integral by selecting a circumference which the radius is r , the expression of the electro-magnetic torque is transformed as:

$$T_{\text{cog}} = \frac{L_{\text{ef}}}{\mu_0} \oint r^2 B_r B_\theta d\theta \quad (3)$$

The two analytical methods use different mathematical methods, energy method is a differential form, while tensor method is an integral form. Maxwell tensor method describes the cogging torque comparative image, while energy method can explore the internal mechanism of the cogging torque more conveniently, which can facilitate the analysis and optimization.

B. Finite element method (FEM)

With the powerful processing capacity of the computer, FEM simulates the actual size of the motor and the specific distribution of the magnetic field. Therefore, it is closest to the actual value of the cogging torque. It can be validated by comparing the finite element method with the measurement results^[5]. In this paper, the cogging torque of the 6-pole 36-slot motor is calculated by using the finite element method.

Cogging torque is expressed as:

$$T_{cog}(\alpha) = \frac{\pi z L_{Fe}}{4\mu_0} (R_2^2 - R_1^2) \sum_{n=1}^{\infty} n G_n B_{r \frac{nz}{2p}} \sin nz\alpha \quad (4)$$

Z —the number of slots; P —the number of pole pairs;

G_n —the amplitude of the n -th harmonic in the Fourier decomposition of the squared ratio permeability;

B_{rm} —the amplitude of the m -th harmonic in the Fourier decomposition of the squared flux density of the air gap; m represents the integer value which can be obtained from $nz/2P$.

$R1$, $R2$ —the annular region surrounded between the two circles with the radii of $R1$ and $R2$ respectively is the solving range of the magnetic energy of the air gap.

For the permanent magnet motors with equal thicknesses of the magnetic steels, the waveforms and expressions of the coefficient G_n and B_{rm} are shown in the figures. Where, h_m represents the thickness of the permanent magnet, $\delta(\theta, \alpha)$ is the distribution function of θ when the relative position between the rotor and the stator is α , θ is the angle that gap length along the circumferential direction of the gap, and θ_s represents the width of the slot.

$$\begin{cases} H(\theta) = \left[\frac{h_m}{h_m + \delta(\theta, \alpha)} \right]^2 = G_0 + \sum_{n=1}^{\infty} G_n \cos nz(\theta + \alpha) \\ G_0 = \frac{z\theta}{2\pi} \left[\frac{h_m}{h_m + \delta} \right]^2, G_n = \frac{2}{n\pi} \left[\frac{h_m}{h_m + \delta} \right]^2 \sin \left(n\pi - \frac{nz\theta_s}{2} \right) \end{cases} \quad (5)$$

$$\begin{cases} B_r^2(\theta) = B_{r0} + \sum_{m=1}^{\infty} B_{rm} \cos 2mp\theta \\ B_{r0} = \alpha_p B_r^2, B_{rm} = \frac{2}{m\pi} B_r^2 \sin m\alpha_p \pi \end{cases} \quad (6)$$

Cogging torque is expressed as:

$$T_{cog} = \frac{\pi z L_{Fe}}{4\mu_0} (R_2^2 - R_1^2) \sum_{n=1, \frac{nz}{2p} \in \mathbb{Z}^+}^{\infty} n B_{r \frac{nz}{2p}} G_n \sin nz\alpha \quad (7)$$

As can be seen from the above formula, the methods weakening the cogging torque are as follows^[6].

1. Adopt the coordination between the poles and the slots (including the use of fractional slot);
2. Adjust the pole arc coefficients;
3. Adjust widths of the slots;

4. Skewing slot;
5. Skewing, step skewing;
6. Pole shifting;
7. Use unequal thicknesses of the permanent magnets;
8. Use unequal widths of the permanent magnets;
9. Different combinations of pole arc coefficients;
10. Different combinations of the widths of the slots;
11. Open auxiliary slots.

Skewing slot is the commonly used method for weakening the cogging torque, but it is difficult to achieve for the direct-drive servo motor which has a short axial length. Moreover, it can affect the operation of core-laminating and the operation of line-embedding^[7]. Therefore, they are commonly used methods for weakening the cogging torque to adjust the coordination of the poles and slots, to adjust the pole arc coefficient, to adjust the width of the slot, and to use unequal thicknesses of the permanent magnets in the designing of the direct-drive servo motors.

III. PRACTICAL METHODS FOR REDUCING COGGING TORQUE

A. Design of weakening the cogging torque of the 36-slot 6-pole motor

Based on the calculation of the actual product, to reduce the cogging torque of the motor most effectively by the feasible methods, three methods including adjusting the pole arc coefficient, using the permanent magnets with non-uniform thickness, and shifting the magnetic pole are used. Based on the methods, the finite element method is employed to set, a variety of programs are compared, and the optimal solution is proposed by the paper.

Table I The basic design parameters of the prototype

D_1 /mm	D_{i1} /mm	D_2 /mm	D_{i2} /mm	L_{ef} /mm
180	116	113	36	140
M_{ic} /mm	M_{d1} /mm	M_{d2} /mm	α_p /mm	PM /mm
5	103	113	0.91	N35SH

Table II The comparison of cogging torque and Inducing different designs

	M_{ic} /mm	α_p	Off /mm	CAM /mNm	Emf /V
1	3.5	0.84	0	229.4	134.5
2	3.5	0.84	5	739.4	137.8
3	3.5	0.85	0	307.8	139.6
4	4	0.85	15	283.4	142.3
5	4	0.87	15	280.7	143.4
6	4	0.87	17	154.7	144.7
7	5	0.91	18	97.35	153.2
8	5	0.91	19	23.43	154.3
9	5	0.91	20	18.45	145.6
10	5	0.91	21	78.15	156.3

Letters are represented as following in table I and table II:

D_I —Outer diameter of the stator; L_{ef} —Core length;

D_2 — Outer diameter of the rotor M_{te} —Magnet thickness
 D_{i1} — Inner diameter of the stator α_p —Pole arc coefficient
 D_{i2} — Inner diameter of the rotor PM —Permanent magnet
 M_{d2} — Outer diameter of the Magnet Off —Offset
 M_{d1} — Inner diameter of Magnet
 EMF —Phase Inducing Voltage
 CAM —Cogging torque amplitude

As can be seen from the table II, the scheme 8 and scheme 9 for reducing cogging torque effect is better, and is relatively easy to implement, In Scenario 9, it is necessary to adjust the number of turns in order to achieve satisfactory emf due to the large degree of unequal thickness pole. Since scheme 9 has the minimum cogging torque and EMF waveform is also better, so the final choice is scheme 9. The prototype and magnetic field is shown Fig.1. Three-phase inducing voltage waveforms is shown in Fig.2. The curve of scheme 9 cogging torque waveforms is shown in Fig.3.

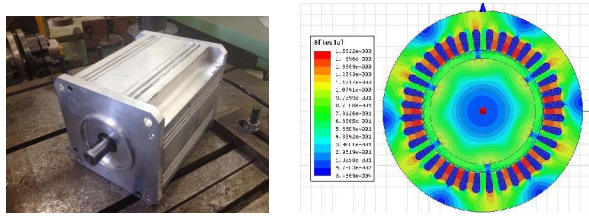


Fig.1. The prototype and magnetic field distribuiton

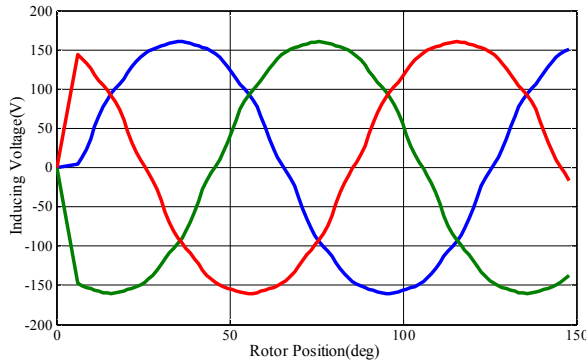


Fig.2. Three-phase inducing voltage waveforms

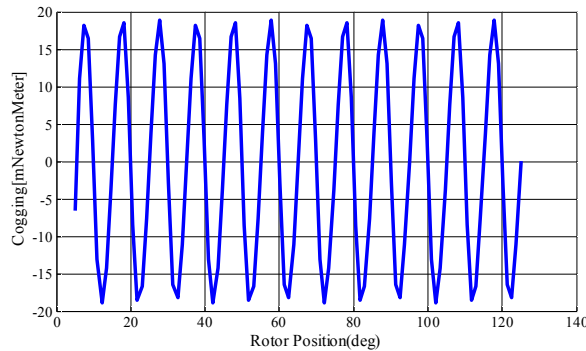


Fig.3. Scheme 9 Cogging torque waveforms

IV. WEAKEN THE IMPACT OF THE COGGING TORQUE OF SOLDER BATH AND TOOTH SATURATION

Since there are solder baths in the stator laminations, the magnetic circuit of the motor will be affected, especially at high saturation of the magnetic circuit of the stator, the solder baths will cause the air gap magnetic energy unevenly distributing in different locations of the rotor, thus the cogging torque reduced before will be increased. This is often ignored during the design of the motor, the pole shift and other conventional methods of weaken the cogging torque can't to achieve satisfactory results^[8].

This paper takes the 36-slot 6-pole motor for example, combining with the finite element software, analyzes the impact of solder baths on the cogging torque in the situation of the magnetic pole shifting, and proposes several ways to reduce the impact. Fig.4 shows the stator piece solder bath of prototype figure schematic diagram.

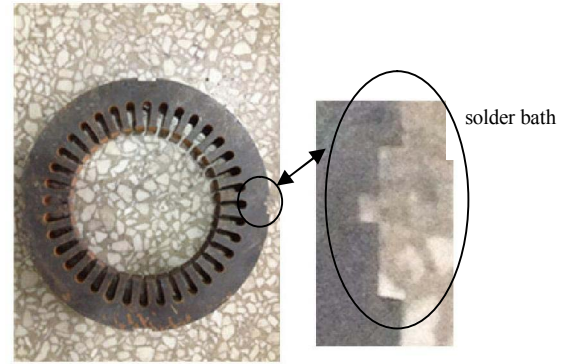


Fig.4 The stator piece solder bath of prototype figure schematic diagram

A. The cogging torque is affected by solder bath

For the 6-pole 36-slot motor, In both cases the analysis by pole uniform and pole shift, cogging torque is affected by solder bath in this study. In the case of the pole shift, cogging torque of the motor with solder bath and without solder bath shown in Fig5.

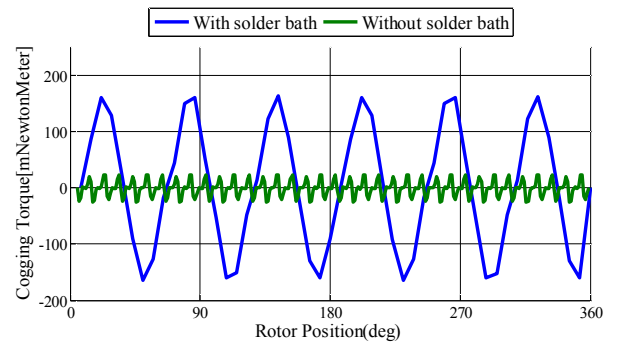


Fig.5 cogging torque of with and without solder bath when pole offset

Under pole offset circumstance, the cogging torque is relatively small. when the solder bath is not opened, cogging torque of the motor rotation has 36 cycles of pulsation and

lower amplitude, about $0.018 \text{ N}\cdot\text{m}$. After opening the solder bath, cogging torque of the motor rotation has 6 cycles of pulsation, the amplitude is about $0.160 \text{ N}\cdot\text{m}$, which is 9 times of original value.

Analysis of the cogging torque generated by the principle that magnetic energy in air gap field varies with the rotor position angle caused, cogging torque represented by the following formula,

$$T_{\text{cog}} = -\frac{\partial W}{\partial \alpha} \quad (8)$$

Where W is air gap magnetic field energy, α is the rotor position angle, by the formula shows that the fastest change in the position of the magnetic energy is the biggest position of the cogging torque.

When there is no weld, the stator yoke portion is uniform, taking no effect on the magnetic circuit of the stator, after notching, solder bath periodically affect the magnetoresistance of the magnetic circuit, this additional periodic changes of magnetoresistance affect flux density, thereby affecting the air gap magnetic. This extra energy is converted into the additional torque which called cogging torque.

The stator yoke flux has relatively high density which has a relatively high saturation in this analyzed prototype, it is transformed into a larger cogging torque because this extra magnetoresistive change is periodically obvious.

B. Weaken The Impact of solder baths

On the basis of pole shift, the cogging torque becomes relatively small and therefore effect of the solder baths is manifested. Weaken the impact of solder baths in order to reduce the cogging torque as possible.

(i) Lower yoke saturation by thickening of the stator yoke

Solder bath periodically affect the magnetoresistance of the magnetic circuit, which is more severe when the yoke saturation is high. Therefore, the saturation level can be reduced by thickening the stator yoke and impact will be weakened. The cogging torque variation can be seen from Fig.5 by thickening of the stator yoke 1mm, 2mm. It is effective that to thicken stator yoke, but reducing the power density of the motor while the yoke is thickened. Fig.6 shows the value of cogging torque in different stator yoke.

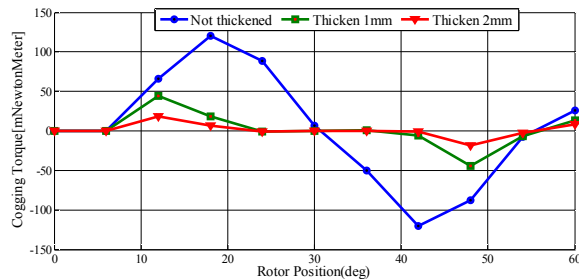


Fig.5 cogging torque in different stator yoke

(ii) Different solder baths and motor poles

4 and 9 welds are analyzed based on the uniform distribution, 5 welds are analyzed based on the uneven distribution, the pitch of the slot and the slot has four 70° and one 80° . Fig.6 shows cogging torque waveform of several cases.

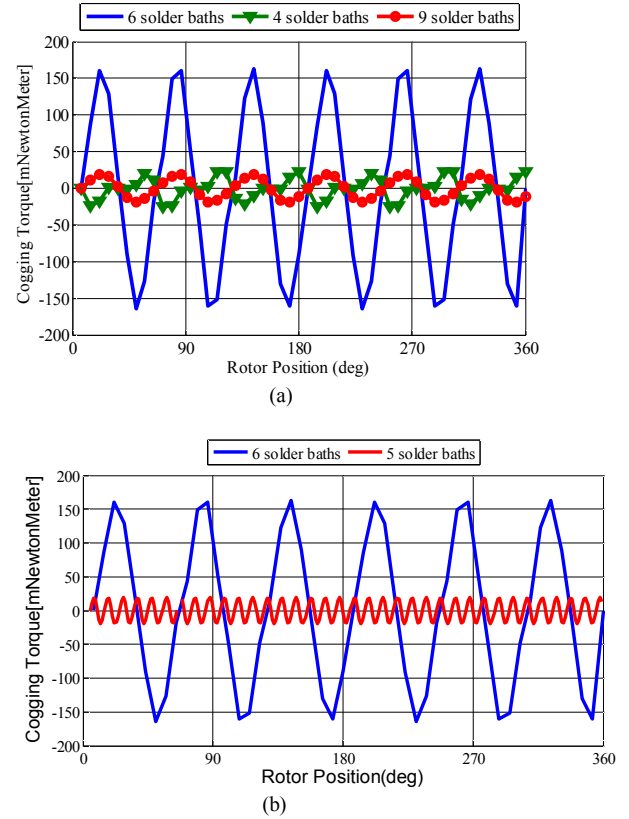


Fig.6. Comparison of cogging torque under different open solder bath method

As can be seen from figure, after using 4, 5, 9 welds, cogging torque value smaller than the original 6 welds. we use 4 welds in terms of this 6-poles and 36-slots motor.

V. CONCLUSION

(i) Using the finite element method to calculate the cogging torque in this article, the basic properties of the cogging torque is analyzed and several methods to weaken are introduced. For the purpose of combining with the manufactures' production practices, researches are carried out in order to weaken the cogging torque.

(ii) For 6-pole 36-slot motor using a magnetic pole shift design, it is analyzed that the solder bath affects cogging torque by finite element method (FEM). The explanation of additional cogging torque is generated by weld and two methods to weaken the weld impact were given.

VI. REFERENCES

- [1] J.F. Gieras, *Permanent Magnet Motor Technology*, 3rd ed., CRC: BocaRaton, 2010, pp. 68-73.
- [2] Z. Q. Zhu, Y. Pang, D. Howe, S. Iwasaki, R. Deodhar, and A. Pride, "Analysis of electromagnetic performance of flux-switching permanent magnet machines by non-linear adaptive lumped parameter magnetic circuit model," *IEEE Transactions on Magnetics*, Vol. 41, No. 11, pp. 4277-4287, Nov. 2005.
- [3] Z. Q. Zhu, Y. Liu, and D. Howe, "Minimizing the influence of cogging torque on vibration of PM brushless machines by Direc Torque Control," *Magnetics, IEEE Transactions on*, Vol. 42, No. 10, pp. 3512-3514, 2006.
- [4] R. Lateb, N. Takorabet, and F. Meibody-Tabar, "Effect of magnet segmentation on the cogging torque in surface-mounted permanent-magnet motors," *Magnetics, IEEE Transactions on*, Vol. 42, No. 3, pp. 442, 2006.
- [5] Xiuhe Wang, Yubo Yang, Dajin Fu, "Study of cogging torque in surface-mounted permanent magnet motors with energy method," *Journal of Magnetism and Magnetic Materials*, pp. 80-85, 2003.
- [6] Xin Zhao, and Hui Liang, "Flux-Weakening Control of Permanent Magnet Synchronous Motor Using in Electric Vehicles," *IPEMC '09. IEEE 6th International Power Electronics and Motion Control Conference*, pp. 1050 - 1054, May 17-20, 2009.
- [7] Byoung-Kuk Lee, Gyu-Hong Kang, Jin Hur, and Dong-Wook You, "Design of Spoke Type BLDC Motors with High Power Density for Traction Applications," in *Proc. Industry Applications Conf.*, vol.2,3-7, no.2, pp.1068-1074, Oct.2004.
- [8] M. Y. Lin, L. Hao, X. Li, X. M. Zhao, and Z. Q. Zhu, "A novel axial fieldflux-switching permanent magnet wind power generator," *IEEE Trans.Magn.*, vol. 47, no. 10, pp. 4457-4460, Oct. 2011.